

# Regenerated Turboshaft Engines for Ground Power Plants Topped with Four-Port Wave Rotors

Fatsis Antonios

Mechanical Engineering Department  
Technological Educational Institute of Sterea Ellada  
34400 Psachna, Greece

**Abstract**—The reduction of fuel consumption in gas turbines, along with the achievement of high levels of performance, remains one of the main goals of the engine's designer. Addition of a heat exchanger (regenerator) is a common method adopted primarily in ground power units where engine's weight and size is not an issue. Moreover, wave rotor technology has shown very promising results in terms of performance enhancement when applied to gas turbines. In this article, detailed calculations are performed for one and two-shaft regenerated gas turbine engines topped with wave rotors built for industrial applications. Having identified the proper placement of the wave rotor in such engines, thermodynamic cycle analysis is implemented, illustrating performance benefits in terms of specific work and specific fuel consumption,

**Keywords**— Wave Rotor, Gas Turbine, Turboshaft, Ground Power Unit, Regenerator, Specific Work, Specific Fuel Consumption.

## I. INTRODUCTION

A wave rotor device is composed of a rotating and a stationary part. The rotating part consists of a number of axial straight blades between two coaxial cylinders forming a drum. The drum rotates inside a stationary casing having two end walls equipped with ports or manifolds, allowing only partial - due to openings on the end walls - inflow and outflow through the blade channels, as illustrated in Fig. 1. Through rotation, the channels' extremities are periodically exposed to the ports located on the upstream and downstream stationary walls initiating compression and expansion waves which are propagated inside the channels. Thus, there is an unsteady pressure exchange between air and exhaust gas by means of pressure waves, as mentioned in [1]. The rotor has axial blade channels, thus assuring port flow alignment.

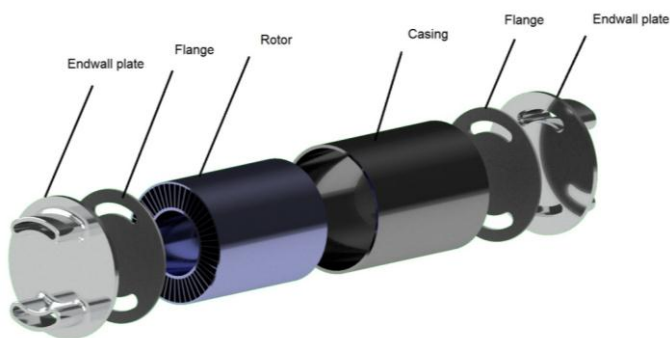


Fig.1. Four-port wave rotor schematic configuration

As a result the power required to keep the rotor at the designed speed is negligible, as mentioned in [2]. It only needs to overcome rotor windage and friction losses. It has been proven in [3] that for

the same inlet and outlet Mach numbers the pressure gain in time-dependent flow devices can be much greater than in the ones operating in steady flow.

When a wave rotor is integrated in a turbomachine, extra air compression is accomplished by means of compression waves formed in the wave rotor channels when hot exhaust gases coming out of the combustion chamber come in contact with air from the compressor. These compression waves are propagated inside the rotor channels in one direction, creating simultaneously expansion waves moving in the opposite direction. Consequently, hot gases are expanded inside the rotor and directed towards the turbine for further expansion. Even though propagation of compression and expansion waves creates a macroscopically unsteady flow pattern inside the wave rotor, the flows entering and exiting the rotor in the ports of the stationary manifolds are almost steady, apart from the fluctuations due to the gradual opening and closing of the rotor channels as they enter and exit the ports. A wave rotor succeeds both compression and expansion within a single component, contrary to the operation of a steady-flow turbomachine.

The configuration assuming unchanged baseline compressor and turbine inlet temperature provides almost the best gas turbine performance enhancement of the wave rotor topped engine. However, the combustor could work under both higher pressure and temperature at the combustor exit, possibly requiring an enhanced structure as well as a fuel injection system, as stated in [4]. Results indicate that the performance of the topped engine is always higher than that of the corresponding baseline engine with the same compressor pressure ratio value. The benefit is greater for lower compressor pressure ratios, whereas for higher ones the benefit diminishes. In fact, for compressor pressure ratios greater than 20, almost no benefit can be obtained. This clearly favors the wave-rotor-topping for small gas turbines with low compressor pressure ratios, as was concluded in [5].

A study aiming to investigate the performance trends of several four-port wave rotor topping configurations was done in [6]. Multi-parametric performance maps were generated by varying component efficiencies, pressure ratios, and temperatures. Even though wave rotor compression efficiency ( $\eta_{WC}$ ) and expansion efficiency ( $\eta_{WE}$ ) are functions of wave rotor temperature and pressure ratios, the above investigation assumed that  $\eta_{WE} = \eta_{WC} = 0.83$ . These values were also applied by other researchers in previous wave rotor studies, such as [7]. It was found that the engine's efficiency is mainly affected by the polytropic turbine efficiency,  $\eta_{PT}$ , in comparison to the polytropic compressor efficiency,  $\eta_{PC}$  and combustion chamber pressure loss,  $\Delta P_{comb}$ . Even though wave rotor topped gas turbine engines seems to be beneficial throughout a wide range of gas turbine sizes, efficiencies, and operating conditions, it was concluded in [6] that the most beneficiary ones are the small gas turbines with low component efficiencies and low temperatures.

Wave rotor benefits were also assessed for the case of a two-spool short range turbofan engine at cruise conditions in [8]. For such engines, the wave rotor is suggested to be placed in the high pressure part of the engine, between the high pressure compressor (HPC) and the high pressure turbine (HPT), being “in parallel” to the combustion chamber.

In [1], a recuperator was proposed to be placed downstream the wave rotor and before the combustion chamber. It was found that the baseline engine with recuperation has much higher efficiency - about twice - and lower specific fuel consumption than the ones of the unrecuperated baseline engine due to the succeeded reduction of heat input in the combustion process.

The design of the transition ducts connecting the wave rotor to compressor, combustion chamber and turbine, seems to have a significant effect on the gas turbine performance. CFD studies were carried out in [9], considering the analysis of the subsonic, unsteady flow exiting the wave rotor with circumferential variation in total pressure and total temperature. Simulations showed that the flow at the exit of the transition ducting system has a total pressure loss of about 7% and a circumferential non-uniformity of total pressure. The latter is expected to influence the turbine performance connected to the wave rotor.

From the literature survey presented above, it is concluded that many efforts have been made to exploit performance benefits when the baseline engine is topped with a four port wave rotor for aeronautical applications. Yet, ground gas turbines for power generation performance benefits have not been analyzed in detail. This study is an original contribution on gas turbine cycle calculations of one-shaft and two shaft regenerated gas turbines with heat exchanger, topped with a four port wave rotor. A performance map comparison between the regenerated topped engines at design point and the baseline regenerated engines provides the data to identify the types of engines and their operating characteristics that benefit mostly of possible integration of a four port wave rotor.

## II. REGENERATIVE GAS TURBINE CYCLES CALCULATIONS

### A. Gas Turbine Regenerators

The technique of adding a regenerator to the basic gas turbine cycle is becoming prominent in our days of high fuel costs and tight reserves. The addition of heat exchanger is widely used in ground based power plants and its benefits in reducing fuel consumption and increasing power output are presented in [10]. Using regeneration, part of the heat available in the exhaust gas stream, otherwise lost, is recovered to preheat air from the compressor outlet before it enters into the combustion chamber. Considering using a heat exchanger with minimum pressure losses and achieving a negligible reduction of power output, the engine requires less fuel consumption thus increasing its thermal efficiency, as shown in [11]. The incorporation of a heat exchanger leads to higher efficiency at low pressure ratios. Additionally, the optimum pressure ratio for the recuperated cycle is much lower than that of the basic. The optimum pressure ratio for maximum specific work is sited between these two pressure ratios according to [12].

However the presence of a heat exchanger in gas turbines for aeronautical applications is prohibited due to its weight, size and flow pattern complexity. In fact the only possibility to fit a heat exchanger in an aircraft engine is to use an air-to-gas compact type. Obviously this problem is obsolete in a ground based plant, where there is no constraint in size and weight and the coolant could be a liquid, [11].

A lot of research efforts have been made on the design of a heat exchanger layout, including material selection, manufacturing technology, and optimization. Based on results reported in the past, a review paper in [13] provides potential heat exchanger designs for gas turbine engines.

### B. Input data

Simple one-shaft gas turbine cycle calculations including a four port wave rotor were presented in detail by [14], so the calculation procedure will not be repeated here. It is important to mention that the calculations of the baseline as well as of the regenerated engine were performed assuming irreversible processes in all the gas turbine components. The thermodynamic model accounts also for cooling the turbine in case  $TIT > 1300$  K by subtracting air flow from the compressor. Typical values of input data are presented in Table I below. For all calculations it was assumed that the values of specific heat at constant pressure and ratios of specific heats are for the air  $C_{pc} = 1005 \text{ J / KgK}$ ,  $\gamma_c = 1.4$  and for exhaust gases

$$C_{ph} = 1150 \text{ J / KgK}, \gamma_h = 1.333$$

TABLE I. BASELINE ENGINE TYPICAL INPUT DATA

Quantity	Symbol, Unit	Value
Ambient pressure	$P_a$ , KPa	101.3
Ambient temperature	$T_a$ , K	288
Intake pressure losses	$\Delta P_m$ (%)	1
Compressor pressure ratio	$R_c$	5 ÷ 30
Combustion chamber pressure losses	$\Delta P_{cc}$ (%)	5
Fuel Low Calorific Value	$FCV$ , MJ/Kg	48.6
Turbine Inlet Temperature	$TIT$ , K	1000 ÷ 1600
Isentropic compressor efficiency	$\eta_{isc}$	0.85
Combustion chamber efficiency	$\eta_{cc}$	0.99
Isentropic turbine efficiency	$\eta_{ist}$	0.90
Heat exchanger efficiency	$n_{HE}$	0.88

### C. Wave Rotor thermodynamic calculations

Typical input data for wave rotor thermodynamic calculations are summarized in Table II.

TABLE II. WAVE ROTOR TYPICAL INPUT DATA

Quantity	Symbol, Unit	Value
Wave rotor pressure ratio	$PR$	1.4 ÷ 2.2
Ducting and leakage losses	$\Delta P_{duct}$ (%)	8
Efficiency of compression processes inside the wave rotor	$n_{WC}$	0.75 ÷ 0.92
Efficiency of expansion processes inside the wave rotor	$n_{WE}$	0.75 ÷ 0.92

Figure 2 illustrates the model used for the thermodynamic calculations of the four-port wave rotor. In this figure it is proposed to place the wave rotor in such a way that its cold inflow port (point 5.0) receives compressed air from the compressor exit and releases it after being further compressed to the heat exchanger cold inlet (point 5.1). The compressed air is preheated inside the regenerator and then directed to the combustion chamber (point 5.2). The hot gases from the combustion chamber enter the wave rotor hot inflow port (point 5.3), come in contact with the cold air being already inside the rotor channels and create compression waves to the air flow, get expanded

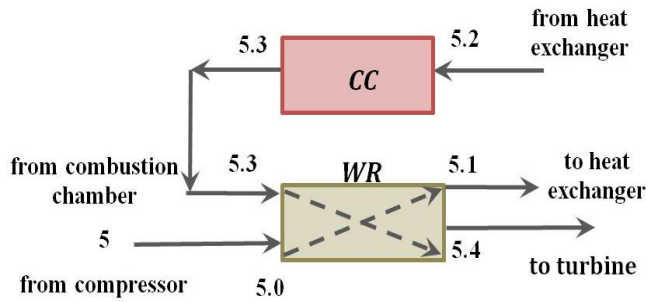


Fig. 2. Symbols used for the four-port wave rotor thermodynamic calculations

and finally directed to the outflow port towards the turbine (point 5.4). The heat exchanger's hot inlet receives the hot gasses from the turbine outflow, enables heat exchange between the compressed air and the hot gasses and releases them to the exhaust of the engine at a lower temperature.

The calculation procedure is the following:

Stagnation temperature at the cold air port of the wave rotor,  $T_{5,0}$

$$T_{5,0} = T_{05} \quad (1)$$

It is assumed that the exit temperature from the outflow port of the wave rotor,  $T_{5,4}$ , equals the turbine inlet temperature,  $TIT$

$$T_{5,4} = TIT \quad (2)$$

Stagnation pressure at the cold air port of the wave rotor  $P_{5,0}$

$$P_{5,0} = P_{05} \cdot \left(1 - \frac{\Delta P_{duct}}{100}\right) \quad (3)$$

Stagnation pressure at the heat exchanger cold part  $P_{5,1}$

$$P_{5,1} = P_{5,0} \cdot PR \quad (4)$$

The stagnation pressure at the outlet port of the wave rotor towards the turbine,  $P_{5,4}$ , is obtained, assuming a linear variation of the pressure ratio  $\left(\frac{P_{5,4}}{P_{5,0}}\right)$  versus the temperature ratio  $\left(\frac{T_{5,4}}{T_{5,0}}\right)$  across the wave rotor, based on experimental and numerical data presented in [15].

Stagnation temperature at the wave rotor exit towards the heat exchanger,  $T_{5,1}$

$$T_{5,1} = T_{5,0} \cdot \left(\frac{PR^{(\gamma_c-1)\gamma_c} - 1}{n_{WC}} + 1\right) \quad (5)$$

Stagnation pressure at the combustion chamber outlet  $P_{5,3}$

$$P_{5,3} = P_{5,2} \cdot \left(1 - \frac{\Delta P_{cc}}{100}\right) \quad (6)$$

Stagnation pressure at the hot inflow port of the wave rotor,  $T_{5,3}$

$$T_{5,3} = \frac{T_{5,4}}{1 - \left[1 - \left(\frac{P_{5,4}}{P_{5,3}}\right)^{(\gamma_h-1)/\gamma_h}\right] \cdot n_{WE}} \quad (7)$$

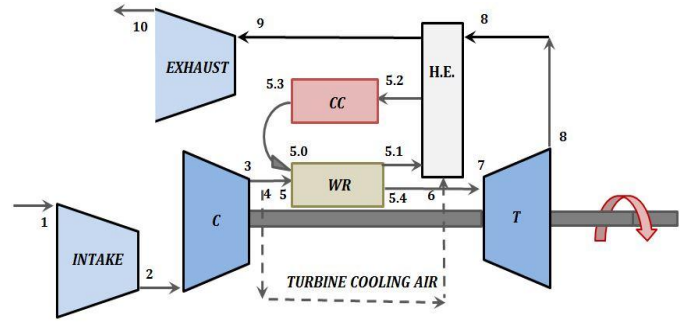


Fig. 3. Four-port wave rotor integrated to a regenerated one-shaft industrial gas turbine

#### D. One-shaft Gas Turbines with Heat Exchanger downstream the wave rotor

One-shaft gas turbines are most suited for fixed speed operation such as base-load power generation. One-shaft gas turbines have the advantage of preventing over-speed conditions due to the high power required by the compressor and can act as an effective brake in case of electrical load loss, as stated in [10].

Figure 3 presents a schematic diagram of a one-shaft gas turbine with heat exchanger including a four-port wave rotor. In this configuration, the heat exchanger transfers heat from the hot gasses at the exhaust of the turbine (point 8) to the compressed air exiting the wave rotor (point 5.1), prior to entering the combustion chamber (point 5.2).

Figure 4 shows the corresponding Temperature - Entropy ( $T$ - $S$ ) thermodynamic diagram of the baseline engine as well as the wave rotor topped regenerated one. Points 2-3-4-7-8 correspond to the baseline engine. Points 2-3-4-5-5.1-5.3-5.4-8' correspond to the topped engine.

Performance curves of various one-shaft regenerated engines at design point conditions without wave rotor (dotted lines) and topped with wave rotor (solid lines) are illustrated in Fig. 5, according to the configuration shown in Fig. 3. Each symbol in Fig. 5 corresponds to a different engine operating at design point conditions. The abscissa of

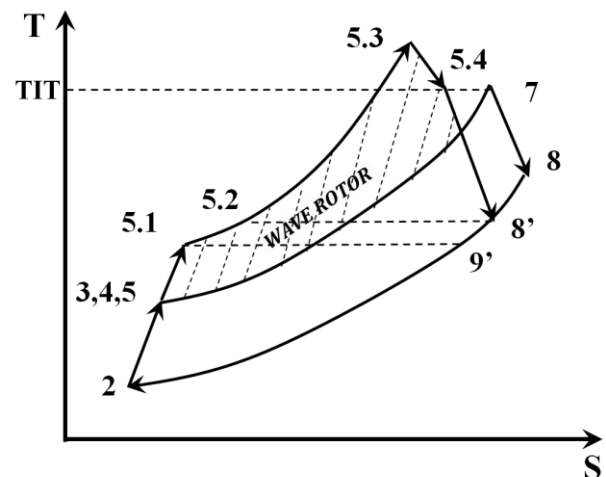


Fig. 4. Thermodynamic diagram temperature-entropy for one-shaft baseline and topped gas turbine engine. Points 2-3-4-7-8 correspond to the baseline engine. Points 2-3-4-5-5.1-5.3-5.4-8' correspond to the topped engine.

the diagram is the specific work ( $w_s$ ) and the ordinate is the specific fuel consumption ( $sfc$ ). These curves are obtained by varying the compressor pressure ratio ( $R_c$ ) from 5 to 30 and the Turbine Inlet Temperature (TIT) from 1000 K to 1600 K. Comparing the performance curves of the baseline regenerated engines (without wave rotor) and the topped regenerated engines with wave rotor, for every single value of TIT, one can observe a significant reduction in  $sfc$  and an increase in  $w_s$ . The general trend of the engines topped with wave rotors is that they operate at lower values of  $sfc$  and at higher values of  $w_s$ . Thus, the performance of the topped engines (continuous lines) is shifted to the right lower part of the diagram. It can be verified as observed in [14], that the shape of curves corresponding to values of TIT > 1200 K resembles to fish hook shape, except for TIT=1000 K and TIT=1100 K, where the curves are widened. Another observation is that for temperatures TIT=1500 K and TIT=1600 K and for compressor pressure ratios ( $R_c$ ) greater than 15,  $sfc$  is remaining nearly constant.

Figures 6 and 7 present a qualitative evaluation of the results obtained in Fig. 5. Figure 6 presents the percentage increase in specific work,  $w_s$ , defined as

$$\% \text{ Increase in } w_s = \frac{w_{s,topped} - w_{s,baseline}}{w_{s,baseline}} \cdot 100 \quad (8)$$

for different values of the compressor pressure ratio (being the abscissa of the diagram) and the turbine inlet temperature. From this figure it can be seen that for each value of  $R_c$ , the increase in  $w_s$  is larger for engines operating at high values of TIT. The maximum gain in  $w_s$ , as defined previously, for an engine with  $R_c=5$  and TIT=1000 K is 12.6%, while for an engine operating at the same  $R_c$  and TIT=1600 K it is becoming 19.4%. For low values of  $R_c$ , there is a greater range of engines with gain in  $w_s$ , operating with TIT from 1000 K to 1600 K. The gain decreases as the  $R_c$  increases and disappears at low TIT values.

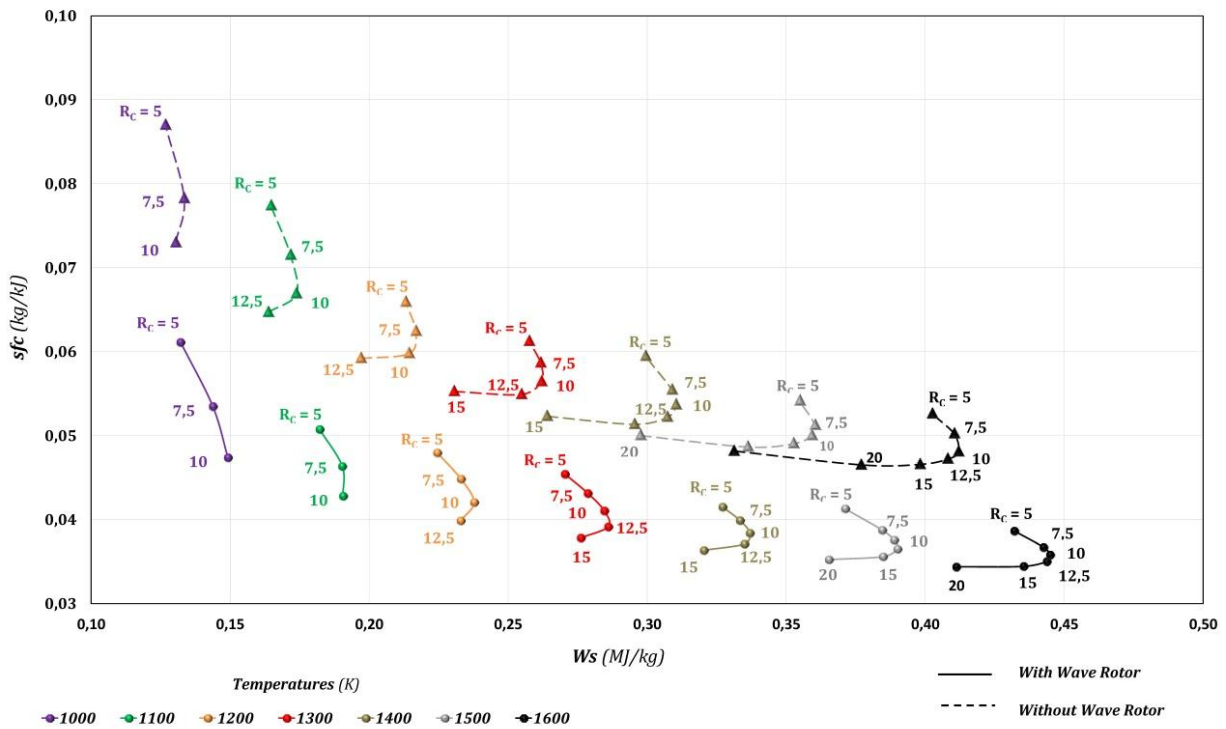


Fig.5. Performance of base line and topped with wave rotor one-shaft gas turbines at design point with heat exchanger, for wave rotor pressure ratio PR=2.2

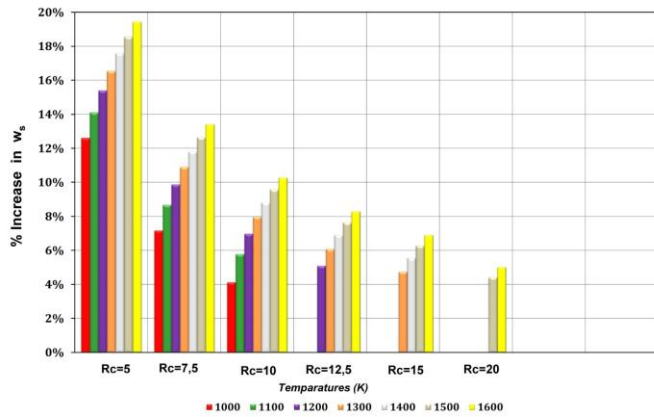


Fig. 6. Gain in specific work between base line and topped with wave rotor one-shaft gas turbines at design point with heat exchanger, for wave rotor pressure ratio equal to 2.2

The percentage reduction in *sfc*, is defined as

$$\% \text{ Reduction in } sfc = \frac{sfc_{baseline} - sfc_{topped}}{sfc_{baseline}} \cdot 100 \quad (9)$$

Figure 7 shows an important reduction in *sfc*, which is higher at lower values of TIT. For  $Rc=5$  and  $TIT=1000$  K the reduction in *sfc* is 54% compared to the untopped baseline engine with heat exchanger. At high values of  $Rc$ , engines with reduction in *sfc*, can operate only at high values of TIT. For example, when  $Rc=15$ , engines can operate only when TIT is greater than 1300 K. For this case, the reduction in *sfc* is 34.8%. Generally, for a given value of  $Rc$ , the largest reduction in *sfc* corresponds to the smallest possible value of TIT that the engine can operate with a benefit. This is why reduction in *sfc* for engines with  $Rc > 15$  corresponds only to high values of TIT.

**E. One-shaft Gas Turbines with Heat Exchanger upstream the wave rotor**

The configuration shown in Fig. 8 is an alternative layout with respect to the positions of the wave rotor and the regenerator in the topped engine assembly. The air at the compressor outlet is preheated at the cold part of the regenerator (points 4 and 5) before entering the wave rotor (point 5.0). There, it comes in contact with the hot gases exiting the combustion chamber (point 5.2) and exchanges energy with them.

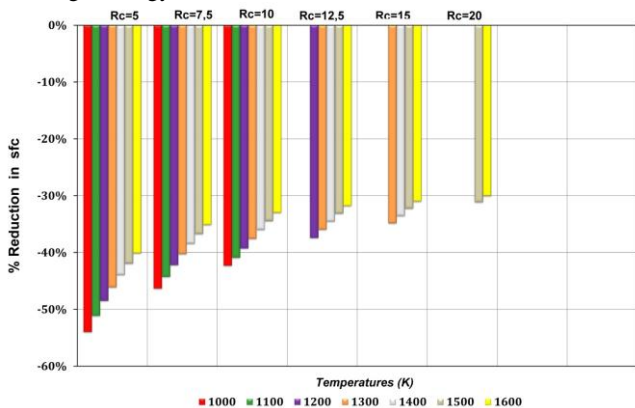


Fig. 7. Reduction in specific fuel consumption between base line and topped with wave rotor one-shaft gas turbines at design point with heat exchanger, for wave rotor pressure ratio equal to 2.2

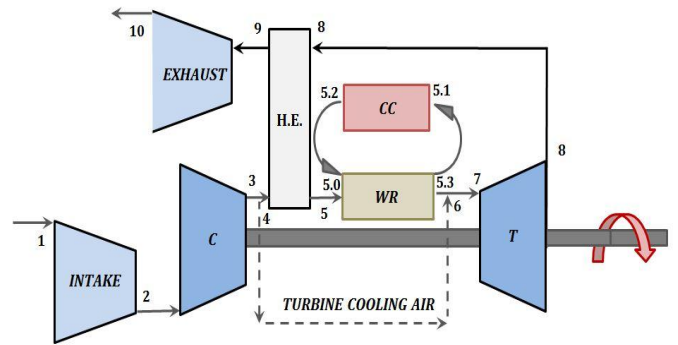


Fig. 8. Four-port wave rotor integrated to a regenerated single shaft industrial gas turbine

As a result there is an air enthalpy increase providing an extra compression before being directed towards the combustion chamber of the gas turbine (point 5.1). Simultaneously, the hot gases inside the rotor are expanded (due to their contact with the air), which results to their enthalpy decrease as they are directed towards the turbine for a further expansion (at point 5.3). At the turbine exit, the pressure of the exhaust gases drops, but their temperature is high enough to exchange heat with the compressed air coming out from the compressor exit when they enter the hot part of the heat exchanger (point 8).

The thermodynamic *T-S* diagram of the baseline engine and the topped one is illustrated in Fig. 9. In this figure the main assumption is that both baseline and topped engines operate under the same compressor pressure ratio and the same turbine inlet temperature (*TIT*). The temperature rise from point 4 to point 5 is due to the heat exchanger. The numbers shown in Fig. 9 correspond to the locations shown in Fig. 8.

Figure 10 illustrates performance curves of various one-shaft engines with heat exchanger according to the configuration shown in Fig. 8, at design point operation topped with wave rotor (solid lines) and without wave rotor (dotted lines). The abscissa of the diagram is the specific work ( $w_s$ ) and the ordinate is the specific fuel consumption (*sfc*). These curves are obtained by varying the compressor pressure ratio from 5 to 30 and the TIT from 1000 K to 1600 K.

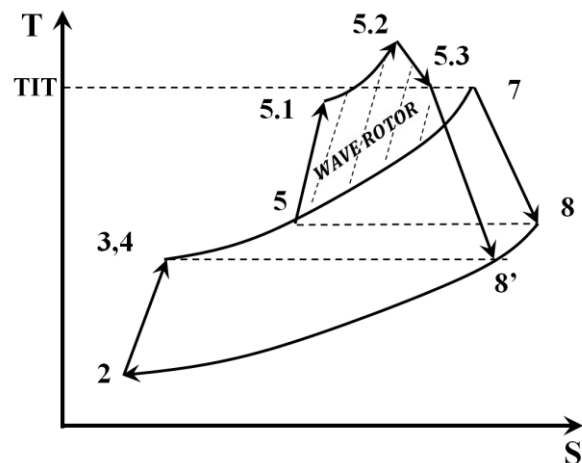


Fig. 9. Thermodynamic diagram temperature-entropy for one-shaft baseline and topped gas turbine engine. Points 2-3-4-7-8 correspond to the baseline engine. Points 2-3-4-5-5.1-5.2-5.3-8' correspond to the topped engine.

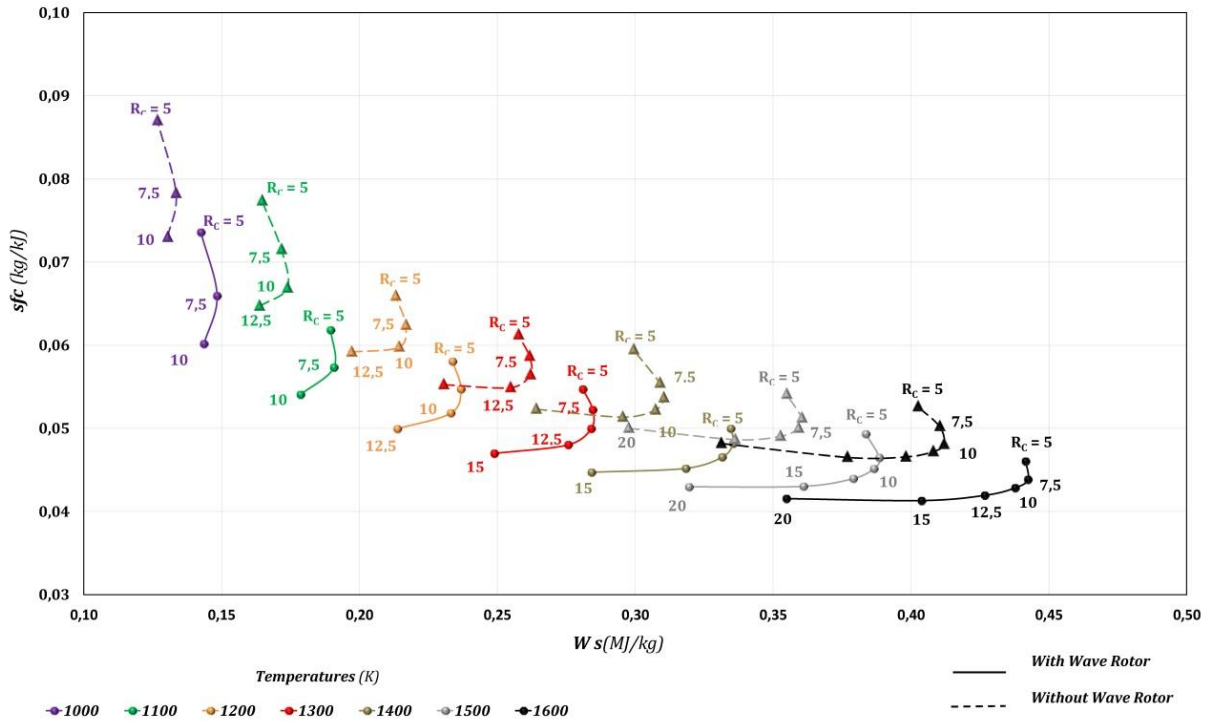


Fig. 10. Performance of base line and topped with wave rotor one-shaft gas turbines at design point with heat exchanger, for wave rotor pressure ratio PR=2.2

Comparing the performance curves of the baseline engines (without wave rotor) and the topped engines with wave rotor, for every single value of TIT, one can observe a reduction in  $sfc$  and an increase in  $W_s$  for the latter ones. The observations from this figure are similar to the observations of Fig. 5, but this configuration shows less significant benefits in terms of  $sfc$  reduction.

Figures 11 and 12 present a qualitative evaluation of the results obtained in Fig. 10. Figure 11 presents the percentage increase in  $W_s$  for different values of the compressor pressure ratio (being the abscissa of the diagram) and the turbine inlet temperature. For reasons of comparison the same scale was used in both Figs. 6 and 11. It can be observed that for each value of  $R_c$ , the increase in  $W_s$  is larger at low values of TIT. The maximum gain in  $W_s$ , as defined previously is 11.1% and it corresponds to  $R_c=10$  and TIT=1000 K. At higher compressor pressure ratios than 10, the gain is decreasing, yet, the highest gain corresponds to the smallest possible operating TIT value.

From Fig. 12, it can be seen a reduction in  $sfc$ , which is bigger at lower values of TIT. For reasons of comparison the same scale was used both in Figs. 7 and 12.

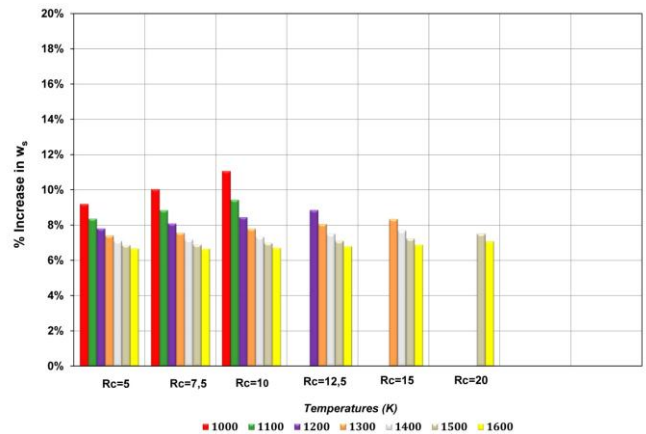


Fig. 11. Gain in specific work between base line and topped with wave rotor one-shaft gas turbines at design point with heat exchanger, for wave rotor pressure ratio equal to 2.2

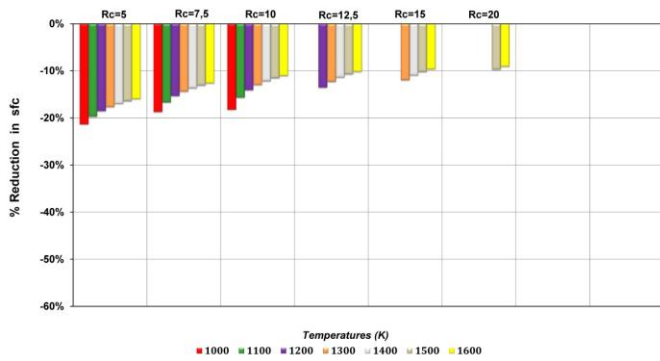


Fig. 12. Reduction in specific fuel consumption between base line and topped with wave rotor one-shaft gas turbines at design point with heat exchanger, for wave rotor pressure ratio equal to 2.2

These figures show the same trend, but in Fig. 12, the reduction in *sfc* is less than half with respect to the previous configuration. For  $R_c=5$ , Fig. 12 shows reduction of 21.3% in *sfc* with respect to the baseline engine with heat exchanger at TIT=1000 K, whereas in Fig. 7 the reduction in *sfc* was 54%. From a given value of  $R_c$ , the largest reduction corresponds to the smallest possible operating value of TIT. As the compressor pressure ratio is increasing, the reduction in *sfc* is even lower with respect to the previous configuration.

#### F. Two-shaft Gas Turbines with Heat Exchanger downstream the wave rotor

Two-shaft gas turbines are also employed in power generation with the power turbine designed to operate at a fixed speed determined by the generator. Unlike one-shaft engines, the gas generator speed varies with electrical load.

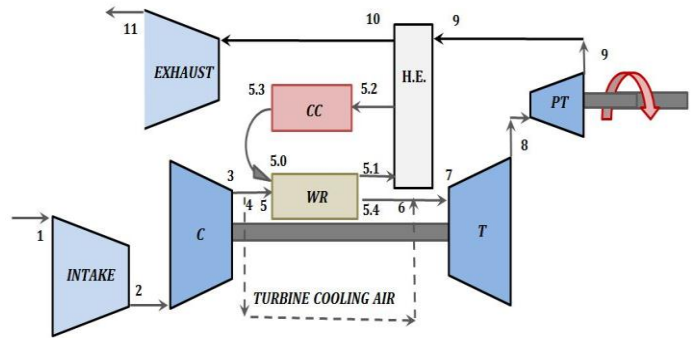


Fig. 13. Four-port wave rotor integrated to a regenerated two-shaft industrial gas turbine

The main advantages with respect to one-shaft engines are the need for lower starting power requirements and better off-design performance. Yet, the disadvantage is that the shedding of the electrical load can result in over-speeding of the power turbine. A layout of a two-shaft regenerated engine, topped with a four port wave rotor is illustrated in Fig. 13.

Figure 14 shows the performance map of regenerated two-shaft gas turbines at design point. Continuous lines depict the results obtained for the topped engines, while dashed lines depict the results of the baseline engines. The input data used - Tables 1 and 2 - is the same as the one for the case of one-shaft regenerated engines (Fig. 5). By comparing Figs. 5 and 14, it can be observed that both types of engines have almost the same performance. However, it must be noted that the performance is slightly better both in terms of  $W_s$  and in *sfc* in the case of the two-shaft engines.

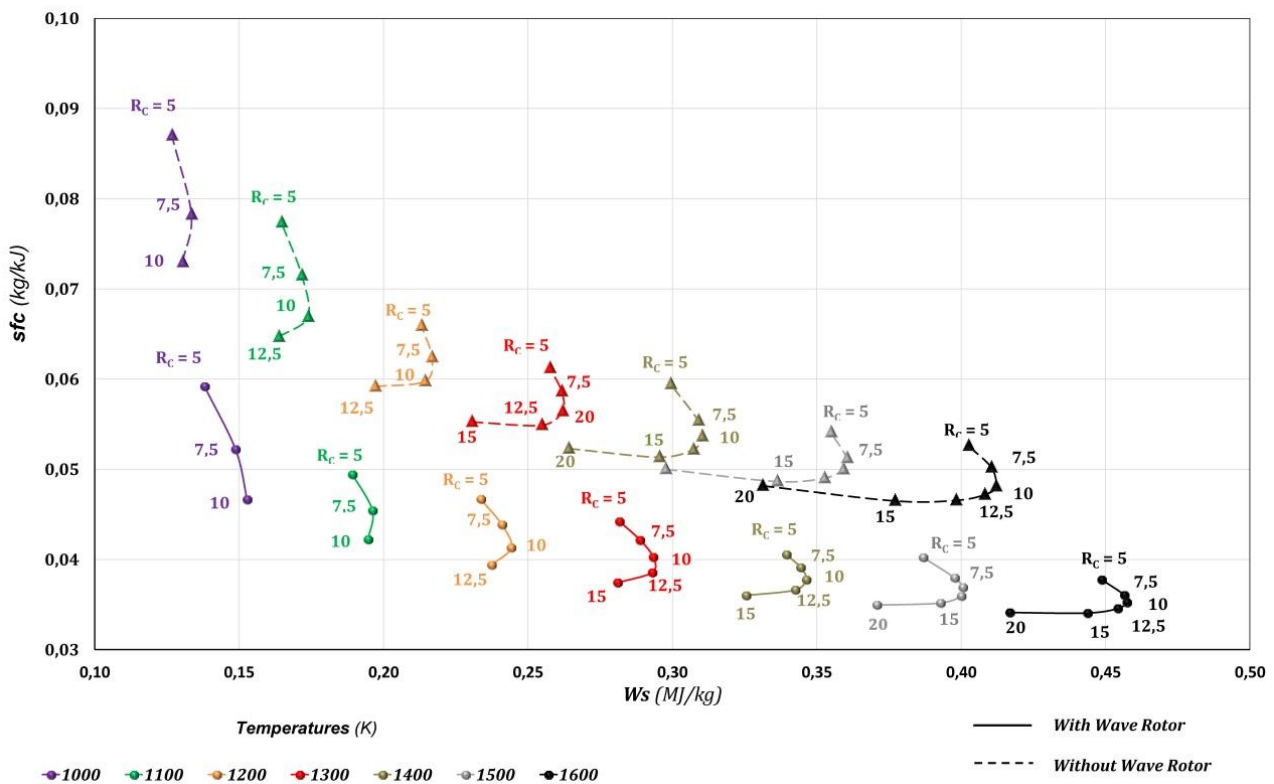


Fig.14. Performance of base line and topped with wave rotor two-shaft gas turbines at design point with heat exchanger, for wave rotor pressure ratio PR=2.2

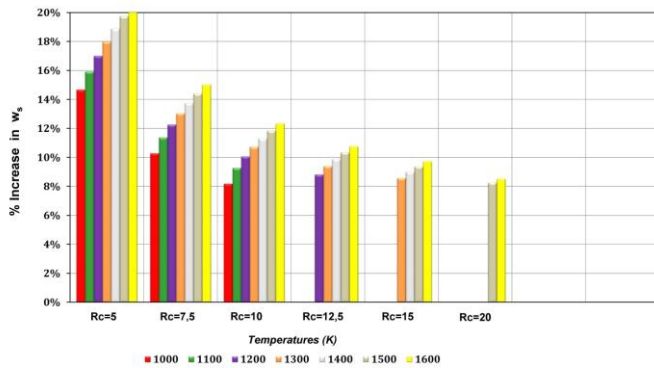


Fig. 15. Gain in specific work between base line and topped with wave rotor two-shaft gas turbines at design point with heat exchanger, for wave rotor pressure ratio equal to 2.2

Figure 15 shows the percentage increase in  $W_s$  with respect to the baseline regenerated engines. As for the case of one-shaft engines it can be observed that for each value of  $R_c$ , the increase in  $W_s$  is larger at high values of TIT. The maximum gain in  $W_s$ , as defined by Eq. (8), is 14.7% when  $R_c=5$  and TIT=1000 K (instead of 12.6% for the case of one-shaft topped regenerated engines), while at  $R_c=5$  and TIT=1600 K it is becoming 20.5% (instead of 19.4% for the case of one-shaft topped regenerated engines). For low values of  $R_c$ , there is a greater range of engines with gain in  $W_s$ , operating with TIT from 1000 K to 1600 K. The gain decreases as the  $R_c$  increases and disappears at low TIT values. From Fig. 16, it can be seen an important reduction in  $sfc$ , which for a given compressor pressure ratio,  $R_c$ , is bigger at lower values of TIT. For  $R_c=5$  and TIT=1000 K the reduction in  $sfc$ , as defined by Eq. (9) is 56.4% (instead of 54% in the case of one-shaft topped regenerated engines). At high values of  $R_c$ , engines can operate at design point only at high values of TIT. For example, when  $R_c=15$ , solution can be acceptable only when TIT is greater than 1300 K. For this case, the reduction in  $sfc$  is 38.5% (instead of 34.8% in the case of one-shaft topped regenerated engines). Generally, for a given value of  $R_c$ , the largest reduction in  $sfc$  corresponds to the smallest possible value of TIT that the engine can operate with a benefit. This is why results for cases that  $R_c > 15$  correspond only to high values of TIT.

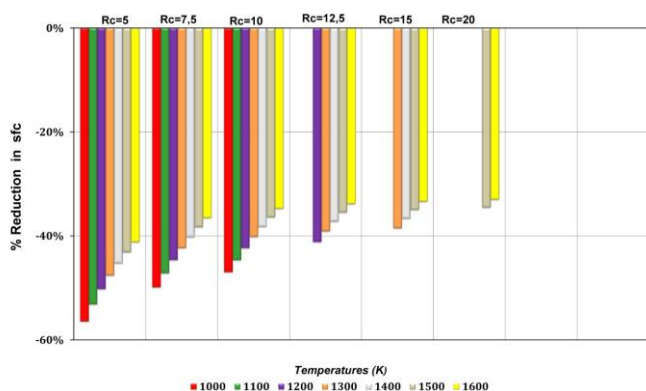


Fig. 16. Reduction in specific fuel consumption between base line and topped with wave rotor two-shaft gas turbines at design point with heat exchanger, for wave rotor pressure ratio equal to 2.2

### III. CONCLUSIONS

In this paper performance benefits for regenerated ground gas turbine engines topped with four-port wave rotors were investigated. Calculations were performed for two typical categories of engines. The first category is the one-shaft engines, where two possible positions of placing the wave rotor were examined. According to the first one, the wave rotor is placed between the regenerator and the combustion chamber. Thermodynamic analysis of the regenerated and topped cycle showed benefits both in terms of gain in specific work,  $W_s$ , and in reduction of specific fuel consumption,  $sfc$ . The second possible position is to place the wave rotor at the exit of the compressor followed by the regenerator. This layout showed significant improvement in the performance of the topped engine and is the one proposed for implementation. Having finalized the most advantageous position of the wave rotor in the regenerated one-shaft engine, calculations were also performed for two-shaft engines at design point. Once more an enhanced performance compared to the baseline engines was verified by the calculations.

The gain in specific work is maximized for engines operating at low values of compressor pressure ratios and high values of turbine inlet temperatures. The reduction in specific fuel consumption is maximized for engines operating at low values of both compressor pressure ratios and turbine inlet temperatures.

### REFERENCES

- [1] Akbari P, Nalim R, Müller, N, "Performance Enhancement of Microturbine Engines Topped With Wave Rotors". ASME Journal of Engineering for Gas Turbines and Power, Vol.128, 2006, pp.190-202.
- [2] Fatsis A, Orfanoudakis N, Pavlou D, Panoutsopoulou A, Vlachakis N "Unsteady flow modelling of a pressure wave supercharger", Proc. IMechE Vol. 220 Part D: J. Automobile Engineering, Vol. 220, 2006, pp. 209-218.
- [3] Weber H.E., "Shock Wave Engine Design", John Wiley and Sons, New York, 1995.
- [4] Akbari P, Müller N, "Performance investigation of small gas turbine engines topped with wave rotors", AIAA Paper No. 2003-4414.
- [5] Akbari P, Müller N, "Performance improvement of small gas turbines through use of wave Rotor topping cycles". ASME Paper No. GT 2003-38772.
- [6] Dempsey E, Müller N., "Performance Optimization of Gas Turbines Utilizing Four-Port Wave Rotors", AIAA Paper No. 2006-4152.
- [7] Fatsis, A., Ribaud, Y., "Thermodynamic analysis of gas turbines topped with wave rotors". Aerospace, Science and Technology, No. 5, July 1999, pp. 293-299.
- [8] Corchero G, Montañés, JL, Pascovici D, Ogaji S., "An insight into some innovative cycles for aircraft propulsion. Proc. IMechE Part G: J. Aerospace Engineering, Vol. 222, 2008, pp.731-747.
- [9] Slater JW, Welch G.E., "Design of a Wave-Rotor Transition Duct", AIAA Paper No. 2005-5143.
- [10] Razak A.M.Y., "Industrial Gas Turbines, Performance and Operability", Woodhead Publishing Limited, Cambridge, 2007.
- [11] Andriani R, Gamma, F Ghezzi U., "Main Effects of Intercooling and Regeneration on Aeronautical Gas Turbine Engines", AIAA Paper No. 2010-6539.
- [12] Horlock J.H. "Advanced Gas Turbine Cycles" Pergamon, Cambridge, 2003.
- [13] Min J.K. , Jeong, J.H. ,Ha, MY, Kim K.S., "High temperature heat exchanger studies for applications to gas turbines. Heat Mass Transfer, Vol. 46, 2009, pp.175-186.
- [14] Fatsis A., "Performance Enhancement of One and Two-Shaft Industrial Turboshaft Engines Topped With Wave Rotors", Int. Journal of Turbo and Jet Engines, Vol. 33, No. 4, 2016.
- [15] Wilson, J., "Design of the NASA Lewis 4-Port Wave Rotor Experiment". AIAA Paper 97-3139.